SMiRT-12 / K. Kussmaul (Editor)

L05/4

A STUDY ON CREEP DAMAGE PARAMETERS IN CREEP CAVITY GROWTH DOMINANT REGION UNDER CREEP-FATIGUE LOADING

F. Ueno, K. Aoto and Y. Wada

Materials Development Section, Systems and Components Division, Oarai Engineering Center, Power Reactor and Nuclear Fuel Development Corporation, Japan

ABSTRACT

Metallographical parameters which can represent the creep-fatigue damage progress under creep damage dominant condition were studied.

A series of creep-fatigue tests which have been interrupted at several fractions of the life were carried out on type 304 stainless steel at a low strain range with long strain hold time. All interrupted test specimens were cut off in an axial plane and observed their microstructures by SEM. The observed cavitation of grain boundaries were quantified using several metallographical parameters. These parameters were compared with the estimated creep damage by a mechanical evaluation model based on linear damage rule. The area fraction of cavity per unit area has a good correlativity with each stage of estimated creep damage.

And the process of cavity nucleation and its growth up to micro-crack initiation along grain boundary was discussed phenomenologically based on the observed data.

1. INTRODUCTION

Development of the creep-fatigue damage evaluation method based on microstructural damage progress is required to improve the reliability of the life prediction of structural material, especially for the extrapolation of the life of actual plant. Also several promising nondestructive methods for creep and creep-fatigue life are studied to develop the life and the residual life evaluation of actual components[1].

The creep damage can be evaluated by the grain deformation measurement under monotonic and high stress level creep conditions[1]. A-parameter[2] and the mean cavity length[3] were proposed for parameters to evaluate creep damage and residual life. By using replicas, such parameters can be measured nondestructively. However, these parameters do not represent both cavity nucleation and its growth simultaneously under creep-fatigue loading.

In this study, the creep-fatigue fracture mode under creep damage dominant condition is discussed in the first. Then the applicability of area fraction of cavity per unit area (AFC)[4] to the creep-fatigue damage evaluation was studied.

And the process of cavity nucleation and its growth up to micro-crack initiation along grain boundary are discussed from the metallographical point of view.

2.CREEP-FATIGUE FAILURE MODE UNDER CREEP DAMAGE DOMINANT CONDITION

Creep-fatigue test results of type 304 stainless steel at 550°C are shown in Fig.1. Creep-fatigue life reduces with increasing of strain hold time at the same strain range.

The regions of 3.5-8.0 mm apart from the main crack on several specimens are observed to measure AFC as shown in Fig.2. Figure 3 shows the relation between AFC and life reduction ratio of creep-fatigue life to fatigue one. In this case, "cavity" includes holes of carbides, ferrites and the other precipitates dissolved or displaced during etching process. But the etching condition of each specimen is the same. It is found out that higher value of AFC can be recognized in the intergranular failure region under the conditions of longer hold time and lower strain range. And this figure shows that the failure mode changes from transgranular to intergranular with increasing of AFC. It is indicated that cavitation of grain boundaries significantly affects to the change of failure mode. In the cases of life fraction of 0.5-1.0 and 0.2-0.5, transgranular and mixed (transgranular and intergranular) failure modes were observed respectively as shown in Fig.3. But in the case of the higher life fraction of below 0.2, intergranular one was observed, and AFC indicated higher value than in the former case.

On the other hand, creep-fatigue life at strain range less than 0.3% with long strain hold time more than several thousand hour have to be estimated for fast breeder reactors (FBRs). Therefore, it is important to evaluate accurately the cavitation in the intergranular failure region to the improvement of reliability of life prediction.

3.INTERRUPTED CREEP-FATIGUE TEST

3.1 EXPERIMENTAL PROCEDURE

In order to clarify cavity nucleation and its growth behavior, five creep-fatigue tests on a solid solution treated type 304 stainless steel have been carried out at 550°C and at 0.5% of total strain range with 10 hours of strain hold time in each cycle. Four of them have been interrupted before failure at 1/50, 1/20, 1/10 and 1/5 of the life. One has been tested to failure. Tested specimens were cut off in an axial plane and the surfaces were etched. Cavities of which diametral size was more than 0.1 micron were observed along grain boundaries by Scanning Electron Microscope (SEM) with 10,000 of magnification.

3.2 EXPERIMENTAL RESULTS

Figure 4 shows the cavitation of the previous five specimens. The number of cavity per unit area (NC) for each size of cavity was measured as shown in Fig.5. At 1/50 of the life, some small cavities less than 2×10^{-2} square micron could be observed. Cavities with the size of more than 2×10^{-2} square micron formed at 1/20 and 1/10 of the life. Till 1/5 of the life, several cavities grew up to the size of more than 10×10^{-2} square micron, and a lot of new cavities less than 2×10^{-2} square micron nucleated simultaneously. On the cross section of the failure specimen, a plenty of small cavities were measured and the size of more than 12×10^{-2} square micron could be observed.

Cavities could be observed already at 1/50 of the life, and they were adjacent to precipitates like carbides. From 1/50 of the life, cavities were growing up. Moreover, new cavities and precipitates could be observed. Especially, the number of cavity was extremely increasing from 1/5 of the life to failure. And it was found out that a number of arrayed cavities along grain boundaries at the failure.

4.DISCUSSION

4.1 Representative metallographical parameter in creep damage dominant region

Figure 6 shows the relation between NC and the state of creep damage which is estimated by a creep-fatigue evaluation method based on linear damage rule (LDR)[5]. NC increases monotonically with the creep damage progress on the logarithmic field. In the case of the mean cavity area, the same relation is shown in Fig.7, and the data band in this figure indicates the width of from minimum to maximum value of cavity area. The mean cavity area approximately keeps a constant through the creep fatigue life. It is indicated that many new cavities form on the grain boundaries successively at the same time when nucleated cavities grow up continuously in creep-fatigue damage progress (see Fig.5). A good correlation between AFC and the creep damage calculated by LDR can be found out as shown in Fig.8. It is noted that AFC can represent the creep-fatigue damage under creep damage dominant condition.

Several creep-fatigue damage evaluation methods based on the cavitation were proposed[6][7]. It is assumed that an distribution of cavity at the early stage of the life are unchangeable, and that all cavities grow up through creep-fatigue cyclings. And the initial cavity size is given as a material constant in some cases[6]. By the observation data in this study, cavities nucleate at the early stage of creep-fatigue condition, but their growth and new cavity nucleations are continued concurrently to the failure. Under creep damage dominant condition, it is required to evaluate both the cavity nucleation and its growth simultaneously at every stage of the creep-fatigue damage through the life.

4.2 Relation between the cavitation and fracture along grain boundary

On both the cross section of interrupted specimen at 1/5 of the life and the failure specimen, internal micro-crack was observed along grain boundary. A SEM photograph of internal micro-crack on the cross section of the failure specimen is shown in Fig.9. The micro-crack propagates along a chain of cavities or precipitate-grain interfaces. Both cavities and precipitates on grain boundary can induce the micro-crack propagation.

The relation between the cavity distribution or location of cavity nucleation, and loading direction is investigated to clarify the process of intergranular fracture.

Figure 10 shows microstructures and schematic illustrations of cavity nucleation and its growth up to micro-crack initiation. At 1/50 of the life, small precipitates of less than 0.1 micron can be observed along grain boundary, and already small cavities can be observed adjacently. In this time, the relation between distribution of cavities on grain boundaries and loading direction cannot be found out. AFC increases remarkably until 1/5 of the life, but after that, AFC increases slowly till failure as shown in Fig.8. From 1/5 of the life, cavity nucleates selectively along grain boundaries which are nearly perpendicular to loading direction. So apparent AFC does not increase with the creep damage progress. We call this phenomena "cavity segregation". Many cracks which are perpendicular to the loading direction can be observed on the cross section of failure specimen because crack propagates along segregated cavities.

Cavity segregation cannot be represented by AFC in the present. Because the distribution of AFC on each grain boundary is not considered individually. To ensure the accuracy of the damage evaluation, consideration of cavity segregation phenomena and its quantitative representation is needed to add on the evaluation by AFC.

5.CONCLUSION

A series of interrupted creep-fatigue tests were conducted, and several metallographical damage parameters were studied to evaluate the creep-fatigue damage under creep damage dominant region. The results are summarized as follows;

(1)The value of area fraction of cavity per unit area (AFC) shows a radical increase under the creep-fatigue loading conditions of longer strain hold time and lower strain range. It coincides with change of failure modes from transgranular to intergranular.

(2)Cavity nucleation and its growth occur simultaneously at every stage of the creep-fatigue damage through the life.

(3)A good correlation between AFC and the creep damage calculated by linear damage rule (LDR) can be found out. And the creep-fatigue damage under creep one dominant condition can be represented by AFC.

(4)On the cross sections of the specimen interrupted at 1/5 of the life and the failure specimen, micro-crack propagates along a chain of cavities and precipitate-grain interfaces. It shows that both cavities and precipitates on grain boundary can induce the micro-crack propagation.

(5)From 1/5 of the life, cavity segregates along the grain boundaries which are nearly perpendicular to the loading direction.

REFERENCES

(1)UENO,F., et al.,(1991); A STUDY OF QUANTITATIVE EVALUATION OF CREEP-FATIGUE DAMAGES BY METALLURGICAL METHOD, Proc. The 1st ASME/JSME Joint Int. Conf. on Nuclear Engineering, Vol.2, pp.351-356

(2)Report of Committee on Reliability Evaluation of Structural Materials, (1991); NON-DESTRUCTIVE EVALUATION OF CREEP AND CREEP-FATIGUE DAMAGE/LIVES OF HEAT-RESISTANT STEELS BY REPLICATION METHOD, The Iron and Steel Institute of Japan(ISIJ) [in Japanese]

(3)IIJIMA,K., et al.,(1988); CAVITY GROWTH DURING CREEP DEFORMATION IN CrMoV STEEL, Current Advances in Materials and Processes, ISIJ, Vol.1, No.6, p.1762 [in Japanese]

(4)TAMURA,K., et al.,(1990); NONDESTRUCTIVE RESIDUAL LIFE EVALUATION TECHNIQUES OF BOILER MATERIALS, Journal of High Pressure Institute of Japan, Vol.28, No.2, pp.91-97 [in Japanese]

(5)AOTO,K., et al.,(1987); AN ANALYTICAL APPROACH TO CREEP-FATIGUE LIFE PREDICTION FOR SUS304, 316 AND 321 AUSTENITIC STAINLESS STEELS, PVP-Vol.123, ASME, pp.43-48

(6)MAJUMDAR,S.,(1991); DESIGNING AGAINST LOW-CYCLE FATIGUE AT ELEVATED TEMPERATURE, Nuclear Engineering and Design, Vol.63, pp.121-175

(7)TOMKINS,B.,(1982); LIFE PREDICTION AT ELEVATED TEMPERATURE, PVP-Vol.59, ASME, pp.149-157

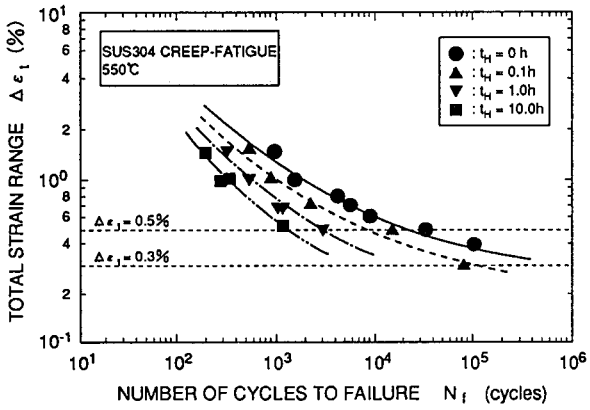

Fig.1 Creep-fatigue life curves at 550°C

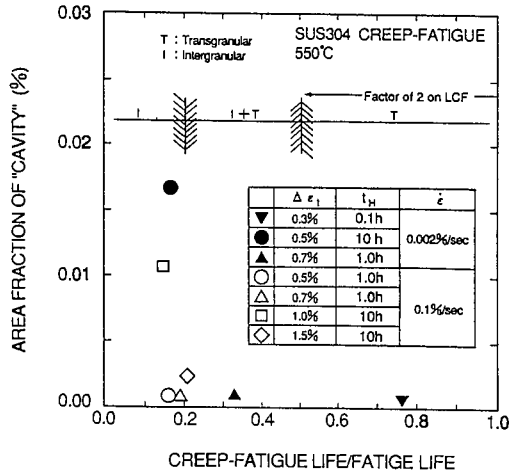

Fig.3 Effect of area fraction of "cavity" on creep-fatigue life reduction

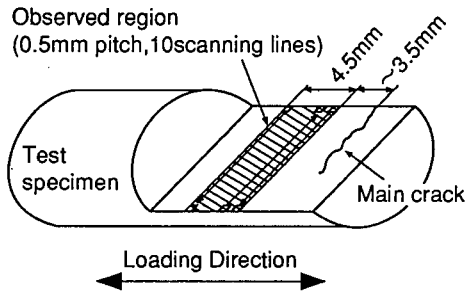

Fig.2 Observed region of cavity in creep-fatigue tested specimen

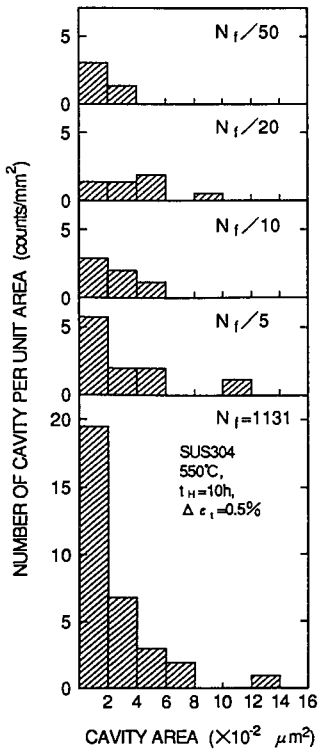

Fig.5 Histograms change of cavity under creep-fatigue loading

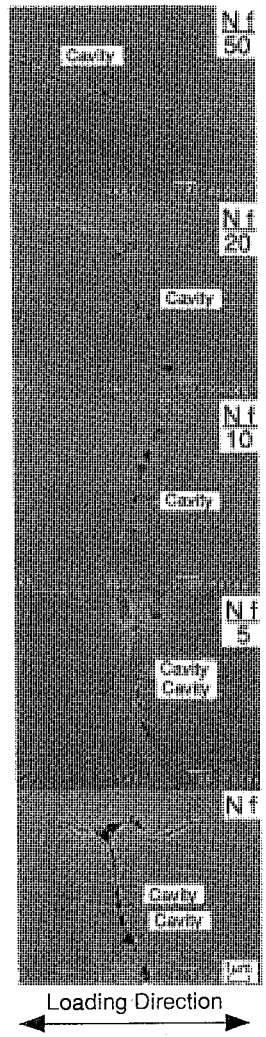

Fig.4 SEM photographs of cavity nucleation and growth along grain boundary (550°C, 10h, 0.5%)

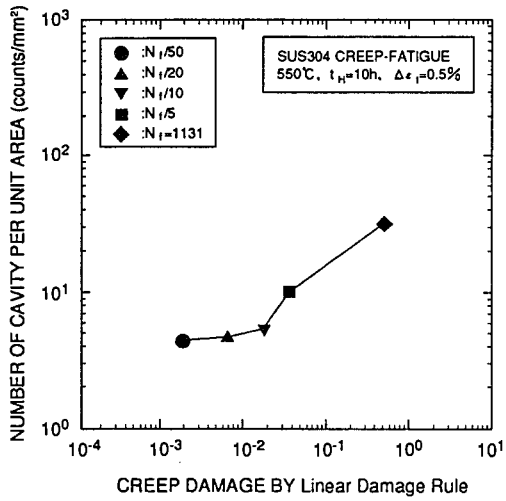

Fig.6 Relation between cavity nucleation behavior and creep damage

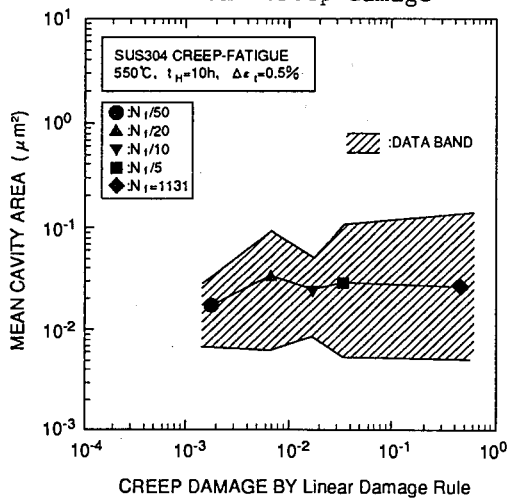

Fig.7 Relation between cavity growth and creep damage

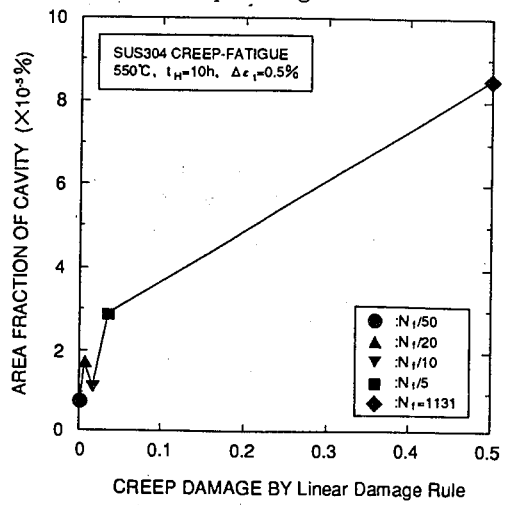

Fig.8 Correlation between area fraction of cavity and creep damage

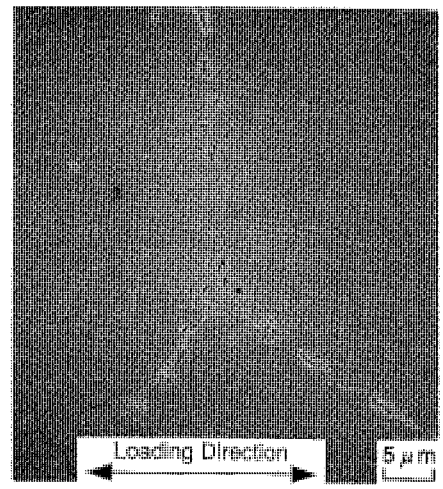

Fig.9 Internal micro crack initiation along grain boundary

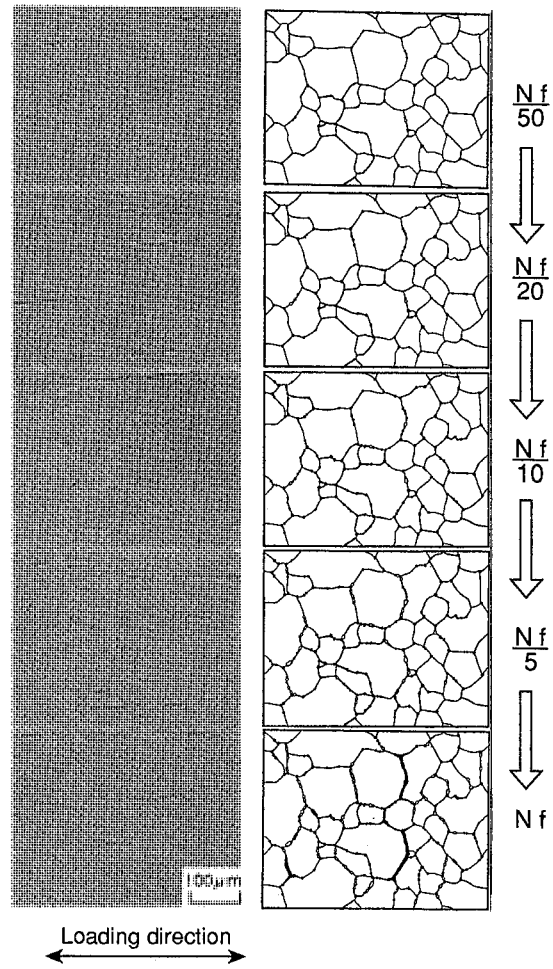

Fig.10 Microstructural damage process under long term creep-fatigue condition

SMiRT-12 / K. Kussmaul (Editor)

L05/5

CREEP-FATIGUE EVALUATION METHOD FOR MOD.9Cr-1Mo WELDMENT

T. Asayama, S. Hasebe, Y. Hirakawa and Y. Wada

Materials Development Section, Systems and Components Division, Oarai Engineering Center, Power Reactor and Nuclear Fuel Development Corporation, Japan

1 INTRODUCTION

It is urged to develop a creep-fatigue evaluation method for weldments of structural materials of the pressure vessels and the coolant systems of future large scale fast breeder reactors (1). The authors have shown that creep-fatigue evaluation of welded joint of 304 stainless steel can be successfully performed based on the concept that the discontinuity of mechanical properties between base and weld metals causes strain concentration within the welded joint (2). Discussed here is a creep-fatigue evaluation method for weldment of Mod.9Cr-1Mo steel which is the most promising candidate material for steam generators of large scale FBRs.

2 EXPERIMENTAL PROCEDURE

2.1 Material and specimen

Two kinds of welded joints were made using hot rolled plate and forged base metals and two kinds of 316 type weld wires by narrow gapped tungsten welding. Post weld heat treatment was performed. Round bar welded joint specimens were taken so that the axis of the specimens were perpendicular to the weld line. The specimens had a diameter of 10mm and a gauge length of 25mm. Hardness distribution in the gauge length before fatigue and creep-fatigue tests is shown in Fig.1. The softest portion is observed in the HAZ.

2.2 Test condition

Strain controlled uniaxial fatigue and creep-fatigue tests were conducted at 550℃ using a servo-hydraulic test machine. Strain rate was 0.1%/s and strain hold time was 10 minutes. Strain waveform was triangular and strain was hold at a tensile peak. Strain range varied from 0.5 to 1.5%.

2.3 Test results

Result of fatigue tests and creep-fatigue tests of welded joints are shown in Fig. 2. Fatigue life of welded joints was a little bit shorter than base metal and was almost the same as weld metal. Creep-fatigue life of welded joints was significantly shorter than that of base and weld metals. Fatigue failure occurred in the base metal and creep-fatigue failure occurred in the weld metal near the interface between base and weld metals.

Figure 3 shows the stress-strain response at mid-life of welded joints. Both base and weld metals showed softening under creep-fatigue

loading. But for welded joints, the softening under creep-fatigue loading was not so clear as for base and weld metals.

3 EVALUATION OF TEST RESULTS BASED ON STRAIN / STRESS CONCENTRATION

3.1 Procedure of evaluation

Procedure of creep-fatigue damage evaluation is illustrated in Fig. 4. The purpose of the procedure is to predict not only fatigue and creep-fatigue life but also location of failure, because location of failure is very important in the utilization of welded joints. First, a welded joint is modeled as a serial combination of three elements, that is, base metal, HAZ and weld metal. Secondly, the mechanical properties, such as cyclic stress-strain response, cyclic softening behavior, creep curve, fatigue strength and creep strength are assumed for each element. Thirdly, the strain concentration and stress concentration are analysed by FE-method. Finally, accumulated fatigue damage and acuumulated creep damage are calculated considering the effect of cyclic softening.

3.2 Model of Mod.9Cr-1Mo welded joint

For 304 welded joint, we have proposed a '2-element model', which is consisted of base metal and weld metal. The discontinuity of mechanical properties between the two elements causes a strain/stress concentration within the welded joint. In the case of Mod.9Cr-1Mo welded joint, HAZ is the softest part in the joint as shown in Fig. 1, where strain concentration may occur. Therefore, '3-element model'(see Fig.4(a)) which is consisted of base metal, weld metal and HAZ was employed in the present study.

3.3 Parameters for analysis

Parameters used for the analysis are summarized in Table 1. The difference of stress-strain response of base metal, weld metal and HAZ are represented by determining σ_p in the following equation for each element (see Fig.4(b)).

$$\log_{10}(\Delta\sigma - 2\sigma_p) = A_0 + A_1 \log_{10}(\Delta\varepsilon - \Delta\sigma/E) \qquad (1)$$

where, $\Delta\sigma$, $\Delta\varepsilon$, σ_p and E are stress range, strain range, proportional limit and elastic modulus, respectively. A0 and A1 are constants. For weld metal, σ_P was determined considering the average trend of the test results. For HAZ, as there was no cyclic stress-strain response data available, it was assumed to be in the range of 0.85 - 1.0 times the value of the base metal, considering the result of hardness distribution test shown in Fig. 1.

3.4 Estimation of strain concentration and stress concentration

Strain concentration and stress concentration were analysed by FE-method using the '3-element model'. Figure 5 shows a typical behavior of strain concentration and stress concentration at the surface of the specimen when a tensile strain of a half of the strain range is imposed. The maximum strain concentration was observed in the base metal about 3-4 mm from the fusion line, although the softest portion was HAZ. It was considered to be the result of plastic constraint on the deformation of HAZ. The maximum stress concentration occurred in the weld metal near the fusion line. As the stress relaxation proceeds and the stress distribution gets less pronounced compared with the beginning of the strain hold period.

3.5 Estimation of fatigue damage and creep damage

Accumulated fatigue damage and creep damage were calculated for base

metal, HAZ and weld metal. Failure of welded joint was defined by the failure of one of the three elements.

Mod.9Cr-1Mo steel is a typical cyclic softening material. In the case of welded joint, base metal, weld metal and HAZ show non-uniform cyclic softening behavior. Therefore, strain / stress concentration behavior depend on the number of cyclic strain. For example, as shown in Fig.6, the location of the maximum strain concentration moves from the fusion line to base metal as repeated strain is imposed. This means that fatigue damage and creep damage per one cycle also depend on the number of cyclic strain.

Hardness distribution after the fatigue test and creep-fatigue test is shown in Fig. 1. It is to be noted that after fatigue and creep-fatigue tests the hardness of HAZ is identical to that of base metal. It is inferred that cyclic softening of HAZ was so small that the hardness of base metal and HAZ coincided during the fatigue / creep-fatigue loading.

Based on the above, a model shown in Fig. 4(c) was assumed. Two assumptions were made, that is, first, cyclic softening is finished in the middle of life and secondly, the ratio of the yield stress between base and weld metal are always constant but that between the base metal and the HAZ changes according to the cyclic strain.

Fatigue damage is calculated as follows: the strain ranges in the base metal, weld metal and HAZ are estimated by FE-analysis using the model shown in Fig.4(c) for all the cycles until failure of welded joint was predicted. The fatigue damage per one cycle df was defined as 1/Nf, where Nf is fatigue life. Creep damage is calculated as follows: the initial strain of stress relaxation in the base metal, weld metal and HAZ were determined by Fig. 4(c) and stress relaxation was calculated by FE-analysis for all the cycles until failure was predicted. The creep damage per one cycle was defined as $\int dt/tr(\sigma)$, where dt and tr are time increment and fracture time, respectively.

Figure 7 shows an example of the accumulation of fatigue damage and creep damage during the cyclic strain at base metal, weld metal and HAZ. Although in the beginning of cyclic strain, fatigue damage is maximum in HAZ, as cyclic softening proceeds, fatigue damage in base metal becomes dominant as a result of change of strain concentration behavior. On the contrary, the behavior of creep damage is almost the same throughout the cyclic strain, that is , creep damage in the base metal is always dominant.

Based on Fig. 7, fatigue life and creep-fatigue life was evaluated based on the linear damage summation rule. Campbell type criterion with the limit value of (Df, Dc)=(0.3, 0.3) was employed for base metal and HAZ, and the Campbell type criterion with the limit value of (Df, Dc) =(0.1, 0.1) was employed for weld metal(3), where Df and Dc are accumulated fatigue damage and creep damage, respectively. As a result, it was predicted that fatigue failure occur in the base metal and creep-fatigue failure occurs in the weld metal. As far as the present study concerns, either fatigue failure nor creep-fatigue failure were predicted to occur in HAZ.

The result of life prediction is shown in Fig. 8. Fatigue and creep-faigue life as well as location of failure was successfully predicted by the model proposed in the present study.

4 CONCLUSION

It was shown that fatigue and creep-fatigue life as well as the location of failure of Mod.9Cr-1Mo welded joint could be successfully predicted by FE-analysis provided the mechanical properties of the elements which compose a welded joint were known.

REFERENCES
(1) Corum, J. M. 1990. Evaluation of Weldment Creep and Fatigue Strength-Reduction factors for Elevated-Temperature Design. Trans. of ASME. J. of Pressure Vessel Technol. 112: 333.
(2) Asayama, T. etal. 1991. Creep-Fatigue Evaluation of SUS304 Welded Joint. SMiRT 11 Transactions Vol.E: 185.
(3) Kagawa, H. etal. 1990. Creep-Fatigue Strength of SUS304 Welded Joints at 550 ℃ and the Evaluation on the basis of Strain Concentration. Materials. 39-440: 503. (in Japanese)

Table 1 List of parameters

Parameter	HAZ	WM
Proportional limit	0.85-1.0xBM	1.15xBM
Fatigue strength	Identical to BM	Average of WM
Creep strength	Identical to BM	Identical to BM
Creep curve	Identical to BM	Average of WM

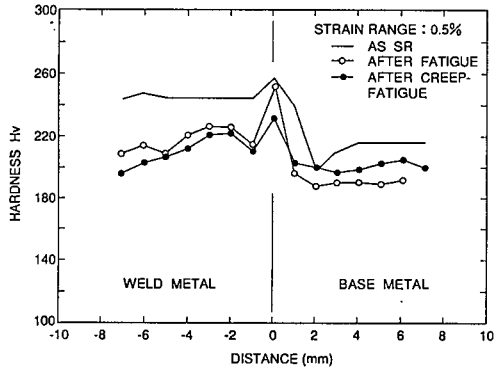

Fig.1 Hardness distribution in gauge length

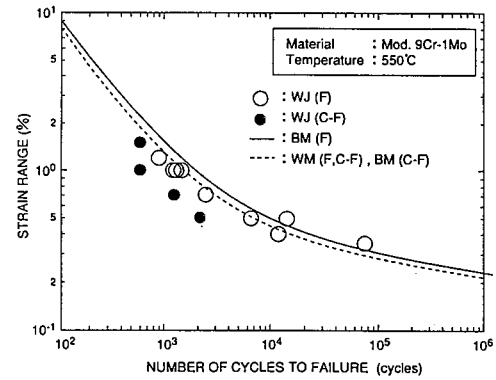

Fig.2 Result of creep-fatigue tests

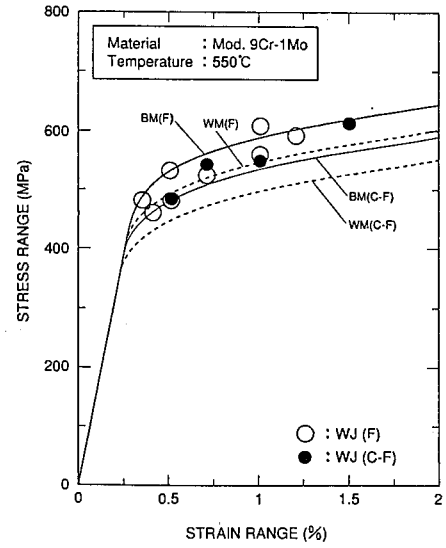

Fig. 3 Stress-strain response

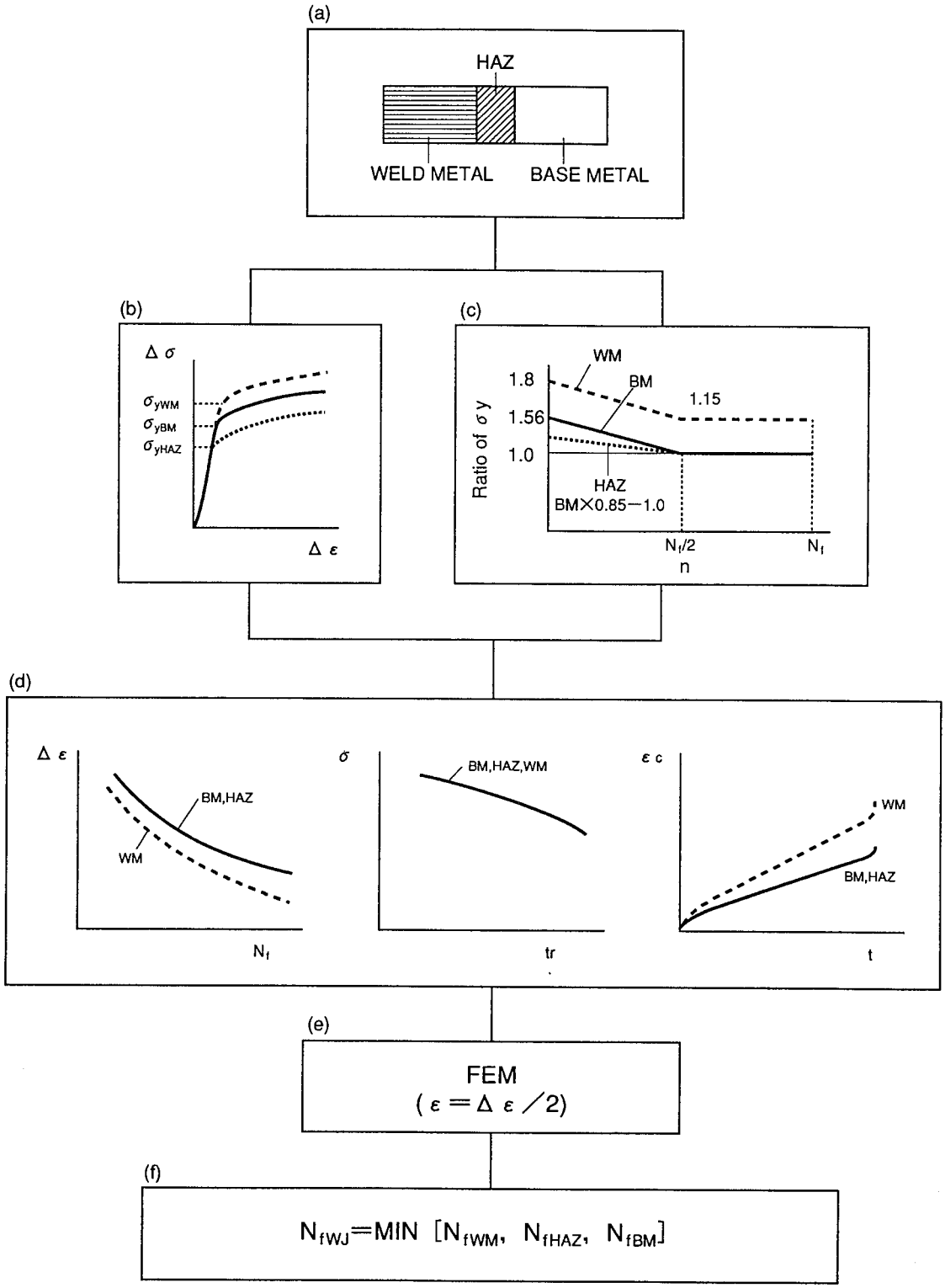

Fig.4 Flow of damage evaluation of welded joint

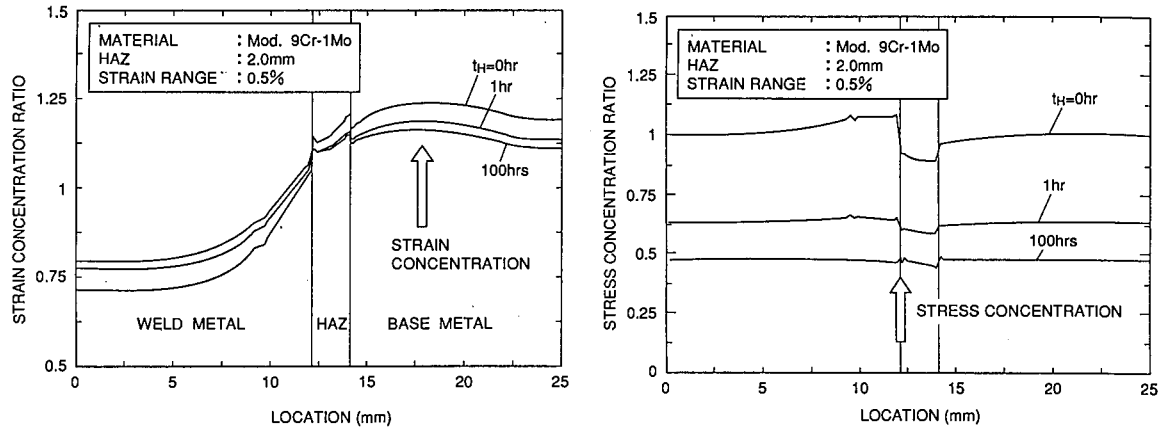

Fig.5 Distribution of strain concentration and stress concentration

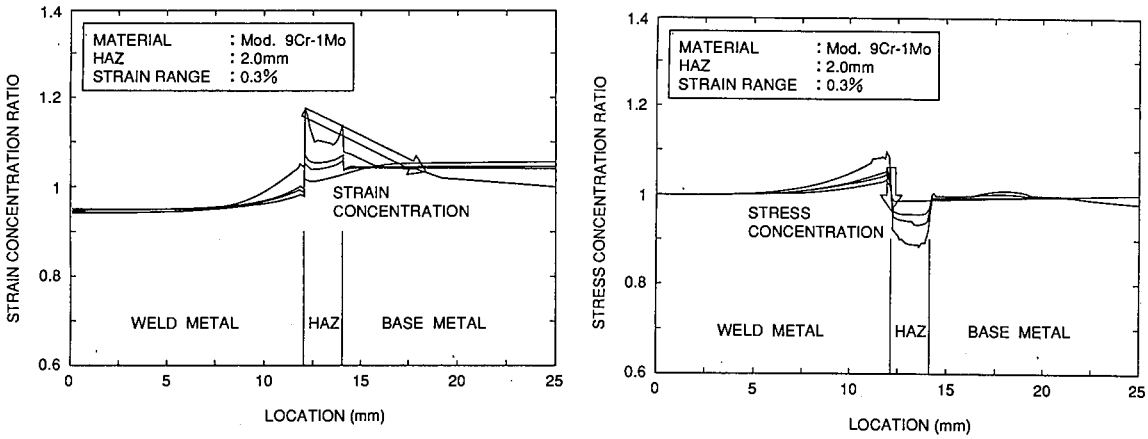

Fig.6 Change of strain / stress distribution during cyclic strain

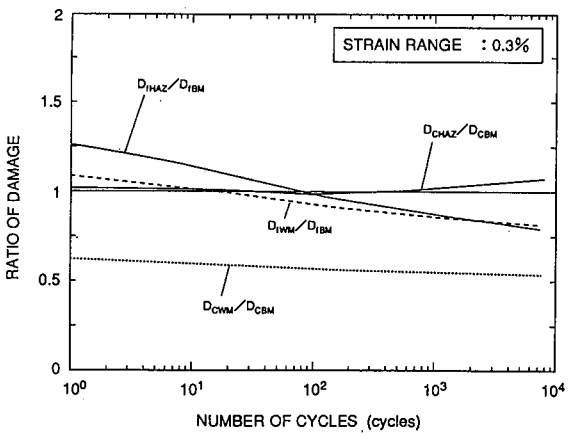

Fig.7 Accumulated fatigue damage and creep damage

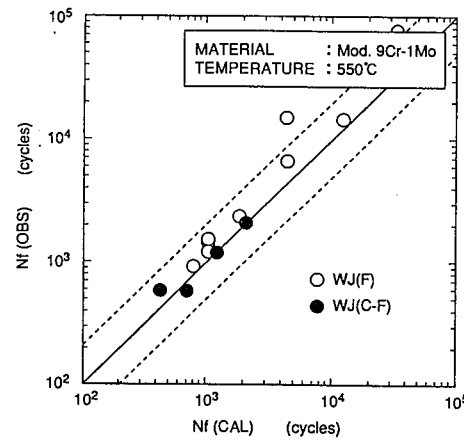

Fig.8 Result of creep-fatigue life prediction